

A Novel Single Stage Push Pull Converter with Integrated Magnetics and Ripple-free Input Current

Rong-Tai Chen
Department of Electrical
Engineering, National Taiwan
University, Taipei, Taiwan.
Email: rtchen@ipmc.ee.ntu.edu.tw

Yung-Yaw Chen
Department of Electrical
Engineering, National Taiwan
University, Taipei, Taiwan.
Email: yychen@ntu.edu.tw

Abstract—This paper presents a novel single stage push-pull boost converter with a improved integrated magnetics and ripple-free input current. It is found that the push pull converter when the duty cycles greater than 50% can simplify the front of boost-type converter to a novel single stage converter. Coupled inductor techniques provide a method to reduce the converter size and weight and achieve ripple-free current. All the magnetic components including input filter inductor and step-down transformer are integrated into a single EI core. The prototype is built to demonstrate the theoretical prediction.

Index Terms—coupled inductors, single stage, integrated magnetics, ripple-free, push-pull boost converter.

I. INTRODUCTION

In recent years, a number of single-stage input current shaping converters have been introduced in [1]-[5]. It is found that many of these topologies can be implemented by combining a two-terminal or three-terminal boost input current shaper cell with DC-DC converter along with an energy storage capacitor in between. The major disadvantages of the conventional two-stage conversion approach are the added cost and the complexity of the two-control loop, two-power-stage nature. The single-stage PFC AC/DC converters that integrated the two power stages into one, thus reducing significantly the component count and cost, have gained much attention in many low-power applications during the past ten years.

In a general sense, the two main switches of push-pull converter operate alternately, with conduction duty cycles of 50% during one complete switching cycle. Conduction overlap of primary switches causes high current spikes during such intervals. In this paper, an improved boost-derived push-pull converter is proposed. It is found that the push pull converter when the duty cycles greater than 50% can simplify the switch of the boost-type converter. Thus, the input current shaper and the push pull converter are integrated together to one single stage. One of the advantages of the overlapping primary switch conduction is the equal division of the inductor current in two switches,

thus reducing their average and rms current levels as well as the primary winding rms current magnitude.

An application of the zero-ripple technique to converter structure is described in [6]. For a basic consideration it seems to be perfect that only by extending a basic converter structure by a defined magnetic coupling of the input and filter inductors a complete elimination of the input current ripple can be obtained. Coupled inductor techniques supply a method to reduce the converter size and weight and achieve ripple-free current. In order to improve efficiency and reduce size, this paper proposes an improved push-pull boost converter with an integrated magnetics. In this structure, all the magnetic components including input inductor, input filter inductor and step-down transformer are integrated into a single EI core.

This paper is organized as follows. Section I introduces the research background and the motivation of this work; Section II briefly reviews basics considerations; Section III proposed an improved push-pull boost converter with integrated magnetics ; Section IV provides experimental results.

II. PRELIMINARY CONSIDERATION

In order to clearly explain the proposed converter, we want to consider the primary concepts in the following.

A. Single stage

There are several interesting single-stage solutions in the state of the art [1]-[5]. Figure 1 shows the pre-regulated DC-DC boost converter with a parallel DC transformer. The switching power circuit (SPC) uses three main switch elements. The two converters are controlled independently to achieve output voltage regulation. The duty cycles of the switches S1, S2, and S3 are D, 50%, and 50% respectively. The duty ratio D may be larger or less than 50%.

If the duty cycles of S2 and S3 are made variable and always greater than 50% i. e. if S2 and S3 have overlapping conduction interval then S1 is no longer needed and it can

be eliminated as shown in Fig. 2.

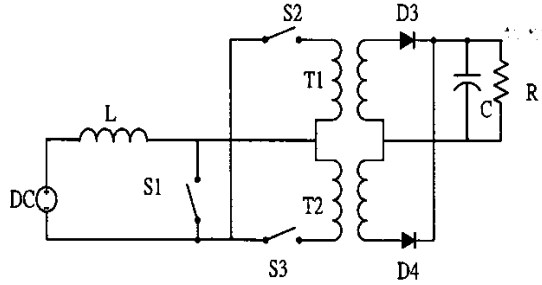


Fig. 1 Pre-regulated DC-DC boost converter:

One of the advantages of the overlapping primary switch conduction is the equal division of inductor current between S1 and S2, thus reducing the switch stress and improving conversion efficiency. The proposed push pull boost converter in Fig. 2 with the duty cycles greater than 50% is a suitable approach for ripple-free input current. This will be verified in the following sections.

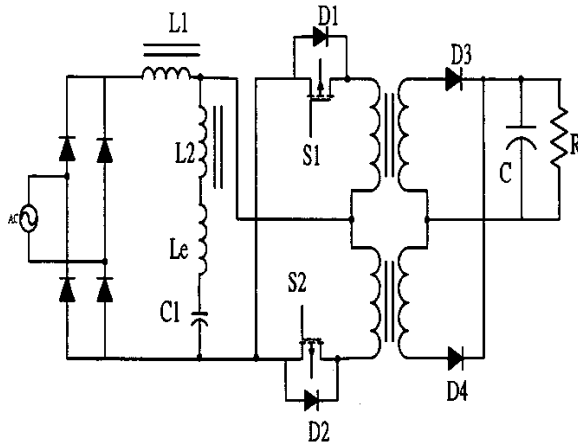


Fig. 2 The proposed push-pull boost converter

B. Zero-Ripple Phenomenon

In order to explain the effect called zero-ripple phenomenon in [6], we want to consider briefly the relationships given for magnetic coupling of the two ports networks shown in Fig. 3. Fig. 3(b) is the equivalent circuit of Fig. 3(a). The elimination of ideal transformer from Fig. 3(b) results in the simple model of Fig. 3(c). The following mathematical model is used to analyze the ripple cancellation.

Let us now make the assumption that is possible to reduce the value of i_1 to zero in our model of Fig. 3(c), and then examine the circuit currents and voltages that result from our assumption. If i_1 is zero, then the AC voltage drop across L1 must also be zero, as illustrated in Fig. 3(a).

These conditions lead to the simplified circuit model of Fig.3(c), where:

$$\frac{N2}{N1} V1 = \left(\frac{N2}{N1}\right)^2 L_M \frac{di2}{dt} \tag{1}$$

$$V2 = Le \frac{di2}{dt} + \left(\frac{N2}{N1}\right)^2 L_M \frac{di2}{dt} \tag{2}$$

Combining Equ.(1) and (2) by the elimination of the common $di2/dt$ factor gives:

$$Le = \left(\frac{N2}{N1}\right) L_M \left(\frac{V2}{V1} - \frac{N2}{N1}\right) \tag{3}$$

The relationship between secondary leakage inductance and that of the core material set by Eq.(3) is important and worth dwelling on for a moment. First of all, recall that this equation was derived based on the premise that no input ripple current existed in our model and, if satisfied, must produce this condition.

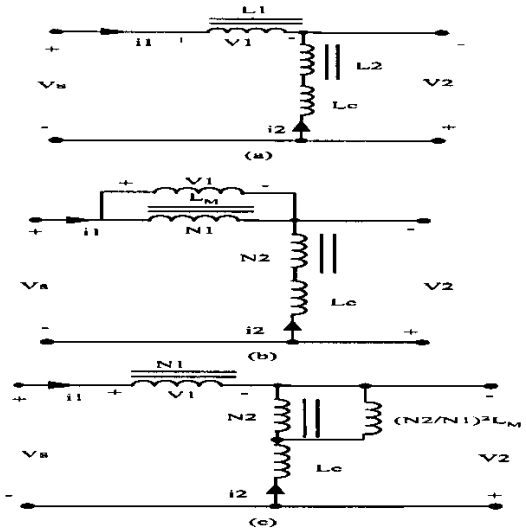


Fig. 3 Two-port network of the magnetic coupling (a) proposed coupling inductor. (b) equivalent circuit of (a). (c) equivalent circuit of (b).

C. Integrate magnetic

The SPC circuits of Fig. 4 are discreted magnetic versions of boost and push pull topologies with transformer isolation, let us now see if we can formulate an easy way to synthesize an integrated magnetic version of Fig.5. To begin, we must first reconstruct the circuit schematics of Fig.4 so as to detail the magnetic aspects of the transformer and inductor components. The schematics the result from this reconstruction process are illustrated in Fig.5 Next, for each of the switching intervals of the converters, a set of equations defining the rate of change of flux in each magnetic component is established [12].

Thus, for the converter of Fig.4 during interval I (S1,S2 ON)

$$\dot{\phi}_L = \frac{d\phi_L}{dt} = \frac{Vs}{NL1} \tag{4}$$

For the converter of Fig.4 during interval II (S1ON ,S2 Off)

$$\dot{\phi}_L = \frac{d\phi_L}{dt} = \frac{V_1}{N_{L1}} - \frac{V_s}{N_{L1}} \quad (5)$$

$$\dot{\phi}_T = \frac{d\phi_T}{dt} = \frac{V_o}{N_{S1}} = \frac{V_1}{N_{P1}} \quad (6)$$

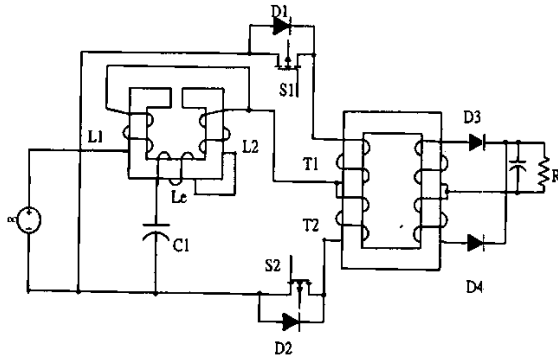


Fig. 4 Discrete magnetics of the proposed push-pull converter

From Eqs. (5) and (6), we can combine them to eliminate the dependent variable, V_1 . Performing this combination gives:

$$\dot{\phi}_T = \dot{\phi}_L \left(\frac{N_{L1}}{N_{P1}} \right) + \frac{V_s}{N_{P1}} \quad (7)$$

Since our goal is to make the inductor a part of the same magnetic assembly that contains the transformer component, it is logical to assume that N_{L1} should be made equal to N_{P1} , so that all of this flux change is contained within one magnetic path or leg of this assembly. Therefore, we arrive at an expression for $\dot{\phi}_T$ as :

$$\dot{\phi}_T = \dot{\phi}_L + \dot{\phi}_s \quad (8)$$

We can interpret Eq.(8) as defining a magnetic assembly in which there are three major flux paths. These general observations permit us now to sketch out a magnetic path arrangement that satisfies the needs of Eq.(8). This is done in Fig. 5.

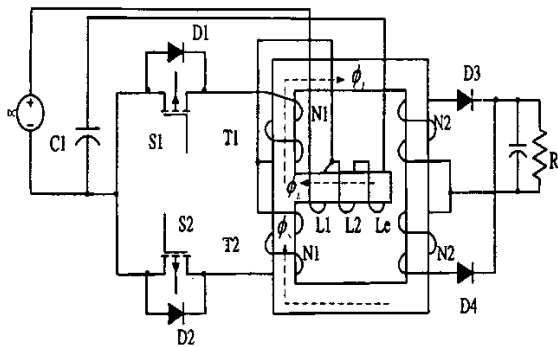


Fig. 5 The integrated magnetics of the proposed push-pull converter

III. PROPOSED PUSH PULL BOOST CONVERTER

This section mainly discusses the steady state and

integrated magnetic properties of the proposed converter. It shows that the proposed boost converter has the same steady-state properties as the conventional boost converter.

A. Principle of operation

The principle of operation in steady-state condition is described with the following assumptions.

- All the switches and components are ideal.
- Transformers T1 and T2 are identical.
- Inductance L1 and L2 are tightly coupled with each other.
- The output voltage V_o is assumed to be constant.

1) Mode 1 ($t_0 < t < t_1, t_2 < t < t_3$)

With the switch S1 and S2 ON, the inductor L1 is grounded. I_s is increased, resulting in energy stored in L1, I_r is increasing and then changes its direction. The diode D1 · D2 is not conducting during this period. The voltage across inductor L1 is the input voltage, V_{in} , and the voltage across inductor L2 is $V_{c1} = V_{in}$.

2) Mode 2 ($t_1 < t < t_2$)

With the switch S1 ON and S2 OFF, I_r releases the energy stored in L1 to the transformer T1. I_r is still keeping its positive direction, however, it is decreasing. The capacitor C1 is charged by I_r . The voltage across inductor L1 is $(V_{in} - V_p)$. The voltage across inductor L2 should be $V_{c1} - V_p = V_{in} - V_p$.

3). Mode 3 ($t_3 < t < t_4$)

With the switch S1 OFF and S2 ON, I_r releases the energy stored in L1 to the transformer T2. The converter action operates the same as mode2.

As a result, the inductances L1 and L2 have the same voltage waveforms during the whole cycle. The voltage relationships of Fig.6, along with the right choice of leakage inductances (L_e) associated with the inductor windings, are the key factors in achieving zero-ripple current at the input of the proposed push-pull converter [8].

B. Steady state analysis

1) Voltage gain

According to the voltage-second balance

$$V_{in} (D - 1/2) T_s = (V_p - V_{in}) (1 - D) T_s \quad (9)$$

$$\text{, where } \frac{V_o}{V_p} = \frac{N_{s1}}{N_{p1}} = \frac{N_{s2}}{N_{p2}} = \frac{1}{n} \quad (10)$$

Thus, the following voltage gain can be derived

$$M_v = \frac{V_o}{V_{in}} = \frac{1}{2(1 - D)n} \quad (11)$$

Considering the power balance $P_{in} = P_o$, that is

$$V_{in} I_s = V_o I_o \quad (12)$$

The current gain is

$$M_I = \frac{I_o}{I_s} = 2(1 - D)n \quad (13)$$

2) DC characteristics

From Fig.6, the average current of i_{L1} and i_{L2} can be derived as follows:

$$I_{avL1} = \frac{1}{4}(2D-1)\frac{V_{in}}{L1}T_s + I \quad (14)$$

$$I_{avL2} = \frac{1}{4}(2D-1)\frac{V_{in}}{L2}T_s - I \quad (15)$$

It can be seen that the presence of the capacitor implies that $I_{avL2} = 0$ in steady state. Leq and K are defined as follows :

$$\frac{1}{Leq} = \frac{1}{L1} + \frac{1}{L2} \quad (16)$$

$$K = \frac{Leq}{RT_s} \quad (17)$$

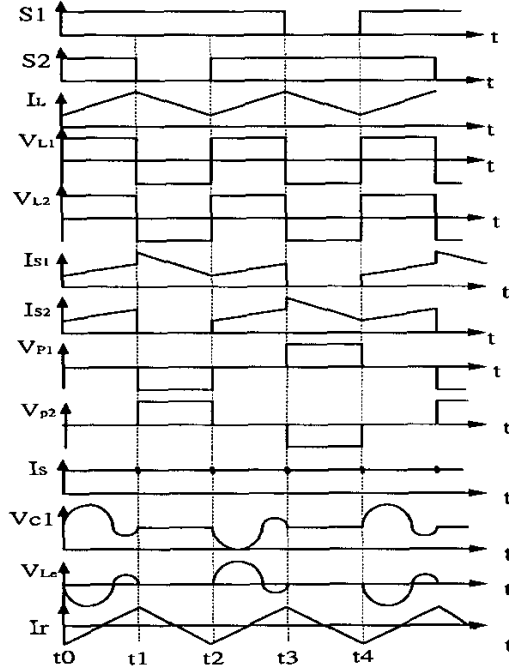


Fig. 6 Main waveforms of the converter in a switching cycle

The output average current flows in the mode2 and mode3, i. e., when the diode is conducting. Therefore

$$I_o = \frac{nV_{in}}{2Leq}(1-D)(2D-1)T_s \quad (18)$$

Using the assumption of 100% efficiency, the average input current can be derived

$$I_s = \frac{I_o V_o}{V_{in}} = \frac{nV_o}{2Leq}(1-D)(2D-1)T_s \quad (19)$$

Summing I_{avL1} and I_{avL2}

$$I_{avL1} + I_{avL2} = \frac{V_{in}}{4Leq}(2D-1)T_s \quad (20)$$

$$= \frac{nV_o}{2Leq}(1-D)(2D-1)$$

An interesting equation can be derived

$$I_s = I_{avL1} + I_{avL2} \quad (21)$$

This means that the averaged input current is equal to

the sum of the currents through the two inductors.

Qualitatively, this must be true since $I_{avL2} = 0$

3) Boundary condition

Considering the power balance again, where

$$P_o = I_o^2 R \quad (22)$$

$$P_{in} = I_s \bullet V_{in} \quad (23)$$

Thus

$$n^2(1-D)^2(2D-1)T_s R = Leq \quad (24)$$

then substituting (17) into (24), that is

$$n^2(1-D)^2(2D-1) = K \quad (25)$$

It can be seen that continuous current mode can be achieved in the proposed topology. The boundary conditions are

$$\frac{1}{2} < D < 1 \quad (26)$$

$$M > \frac{1}{n} \quad (27)$$

$$K > 0 \quad (28)$$

4) Semiconductor devices stress

The switch average current is

$$I_{avS1} = I_{avS2} = \frac{V_{in}T_s}{2Leq}\left(D - \frac{1}{2}\right)\left(\frac{3}{2} - D\right) \quad (29)$$

The diode average current is

$$I_{avD3} = I_{avD4} = \frac{nV_{in}T_s}{2Leq}(1-D)(2D-1) \quad (30)$$

The switch peak current is

$$I_{pkS1} = I_{pkS2} = \frac{V_{in}T_s}{2Leq}(2D-1) \quad (31)$$

According the previous analysis, Fig. 7 shows some characteristic curves for the proposed converter.

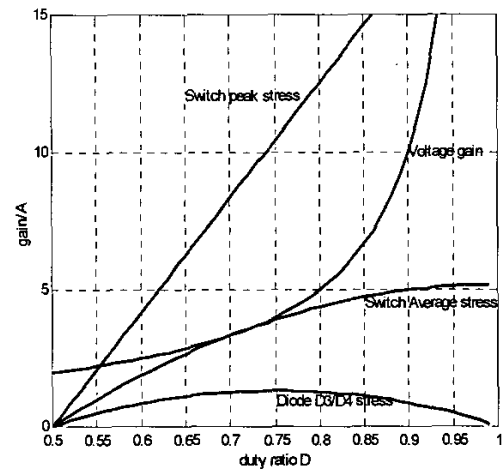


Fig. 7. Characteristic curves for the proposed converter.

C. Derivation of the integrated magnetics

A novel magnetic integration approach is proposed for the push-pull boost converter as follows. The current

directions are defined as in the equivalent electrical circuit shown in Fig.8.

Fig.8 (a) shows the reluctance model for the proposed magnetic circuit. The electrical circuit model can be derived from the reluctance model by using the principle of duality, as shown in Fig. 8 (b). The circuit of Fig. 8 (c) results from scaling step with N_p designated as the reference winding. The scaled permeances are then replaced by inductances. From the reluctance circuit shown in Fig. 8(a), the fluxes in the cores can be derived in the form of reluctances and MMF sources, as follows:

$$\phi_p = \frac{\mathcal{R}_c + \mathcal{R}_g}{\mathcal{R}_c(\mathcal{R}_c + 2\mathcal{R}_g)} N_p \cdot i_p - \frac{\mathcal{R}_g}{\mathcal{R}_c(\mathcal{R}_c + 2\mathcal{R}_g)} N_s \cdot i_s \quad (32)$$

$$\phi_s = \frac{-\mathcal{R}_g}{\mathcal{R}_c(\mathcal{R}_c + 2\mathcal{R}_g)} N_p \cdot i_p + \frac{\mathcal{R}_c + \mathcal{R}_g}{\mathcal{R}_c(\mathcal{R}_c + 2\mathcal{R}_g)} N_s \cdot i_s \quad (33)$$

Where, \mathcal{R}_c and \mathcal{R}_g represent the reluctances of the outer and center legs, and i_p and i_s are the total winding currents reflected to primary and secondary of the transformer, respectively. According to Farady's Law, and that the mutual inductance between L_p and L_s is M , and coupling coefficient is k , the relationship between inductances and reluctances can be derived as follows:

$$L_p = \frac{(\mathcal{R}_c + \mathcal{R}_g) N_p^2}{\mathcal{R}_c(\mathcal{R}_c + 2\mathcal{R}_g)} \quad (34)$$

$$L_s = \frac{(\mathcal{R}_c + \mathcal{R}_g) N_s^2}{\mathcal{R}_c(\mathcal{R}_c + 2\mathcal{R}_g)} \quad (35)$$

$$M = \frac{\mathcal{R}_g N_p N_s}{\mathcal{R}_c(\mathcal{R}_c + 2\mathcal{R}_g)} \quad (36)$$

$$k = \frac{\mathcal{R}_g}{\mathcal{R}_c + \mathcal{R}_g} \quad (37)$$

As can be seen from Eq. (35) and (36), in the proposed integrated magnetic structure, the coupling coefficient for the transformer is close to one. Two coupled windings still have a certain amount of leakage inductance. In practice, the reluctances from the magnetic material influence the value of \mathcal{R}_c and \mathcal{R}_g .

IV. EXPERIMENT RESULT

The new push-pull boost converter was implemented, with the following specifications: output power $P_o=80$ W ; input voltage $V_{in}=25$ V; output voltage $V_p=35$ V; switching frequency $f_s=200$ Khz.

The switch conduction sequences of the proposed converter are shown in Fig. 9. It can be seen that the duty cycles greater than 50%. The line current and line voltage are shown in Fig. 10. It can be seen that the ripple is almost zero. Fig. 11 shows the voltage across capacitor $L1 \cdot L2$. It has the same wave. The corresponding line-current harmonics are shown in Fig. 12. The harmonic limits for IEC 1000-3-2 class D standard are also given in Fig. 12. It satisfies the standard with enough margins. The efficiency of the power stage of the converter is shown in Fig. 13. The maximum value at full load is 90%.

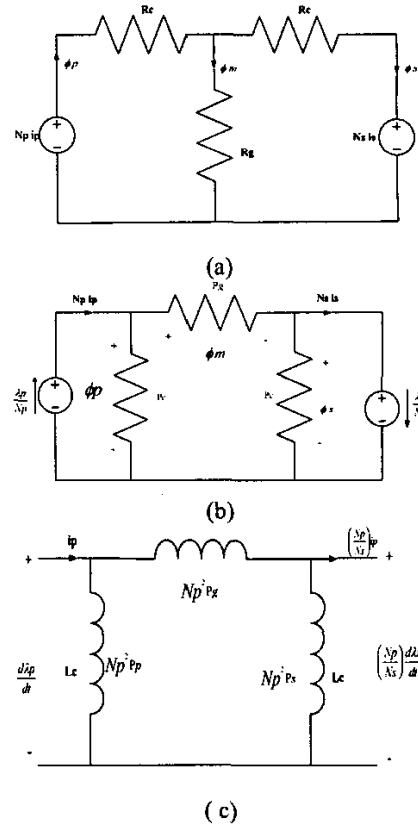


Fig. 8 (a) The reluctance model of proposed magnetic circuit (b) model (a) by using the principle of duality (c) model (b) of scaling step with N_p designated as the reference winding.

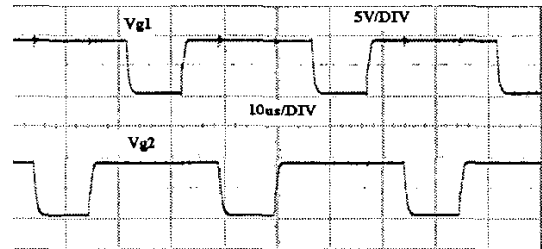


Fig. 9 Measured MOSFET gate voltage (V_{g1} , V_{g2}) waveforms.

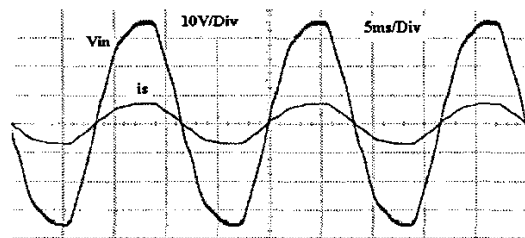


Fig. 10. Measured the line voltage (V_{in}) and line current (i_s) waveform with input current shaper

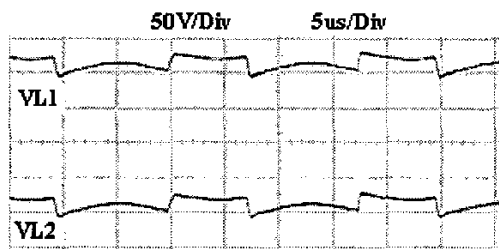


Fig. 11 Experiment results of the voltage across inductor

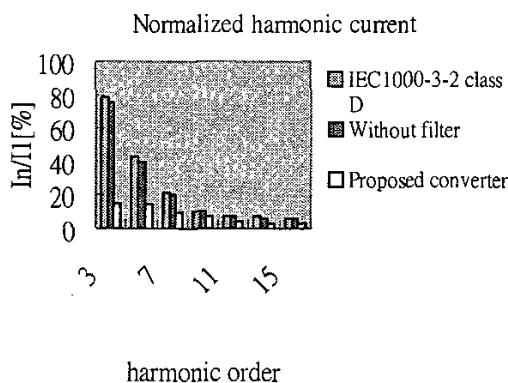


Fig. 12 The corresponding line-current harmonics.

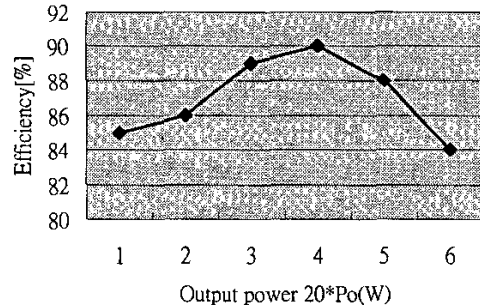


Fig. 13 The efficiency of the proposed converter

V. CONCLUSIONS

A novel simple single-stage push-pull AC/DC converter has been introduced. This converter can achieve small converter size and zero-input current using coupled inductor techniques. The proposed circuit is of simple topology and control strategy. It has several advantage such as lower switch and diode stress, lower stresses on capacitor C1. This makes the conduction and switching losses low and may result in a high efficiency. It is proved that the proposed boost converter has the same steady-state properties as the conventional boost converter. It is proved that the proposed

boost converter has the same steady-state properties as the conventional boost converter. Blending of inductors and transformers of SPCs into single magnetic systems can be very advantageous, often resulting in converter designs of lower cost, weight, and size than their discrete magnetic counterparts. Conversion performance can also be improved and component stresses reduced, provided the integration process is well thought out and executed properly.

VI. REFERENCES

- [1] C. Qiao, and K. M. Smedley, "A topology survey of single-stage power factor corrector with a boost type input-current shaper," *IEEE Trans. Power Electron.*, vol. 16, pp. 360-368, May. 2001.
- [2] O. Garcia, J. A. Cobos, P. Alou, and J. Uceda, "A simple single-switch single-stage AC/DC Converter with fast output voltage regulation," *IEEE Trans. Power Electron.*, vol. 17, pp. 163-171, March. 2002.
- [3] L. Huber, and M. M. Jovanovic, "Single-stage single-switch input-current-shaping technique with fast-output-voltage regulation," *IEEE Trans. Power Electron.*, vol. 13, pp. 476-486, May. 1998.
- [4] Q. Zhao, F. C. Lee, and F. Tsai, "Voltage and current stress reduction in single-stage power factor correction AC/DC converters with bulk capacitor voltage feedback," *IEEE Trans. Power Electron.*, vol. 17, pp. 477-484, July. 2002.
- [5] L. Huber, J. Zhang, M. M. Jovanovic, and F. C. Lee, "Generalized topologies of single-stage input-current-shaping circuits," *IEEE Trans. Power Electron.*, vol. 16, pp. 508-513, July. 2001.
- [6] J. Wang, W. G. Dunford, and K. Mauch, "Analysis of a ripple-free input-current boost converter with discontinuous conduction characteristics," *IEEE Trans. Power Electron.*, vol. 12, pp. 684-694, July. 1997.
- [7] J. Abu-Qahouq, and I. Batarseh, "Unified steady-state analysis of soft-switching DC-DC converters," *IEEE Trans. Power Electron.*, vol. 17, pp.684-691, September. 2002.
- [8] P. Xu, M. Ye, P. L. Wong, and F. C. Lee, "Design of 48V voltage regulator modules with a novel integrated magnetics," *IEEE Trans. Power Electron.*, vol. 17, pp. 990-998, November. 2002.
- [9] S. Hamada, and M. Nakaoka, "A novel zero-voltage and zero-current switching PWM DC-DC converter with reduced conduction losses," *IEEE Trans. Power Electron.*, vol. 17, pp. 413-419, May. 2002.
- [10] C. M. Duarte, and I. Barbi, "An improved family of ZVS-PWM active-clamping DC-to-DC converters," *IEEE Trans. Power Electron.*, vol. 17, pp.684-691, January. 2002.
- [11] B. K. Bose, *Power Electronics and AC Drives*. Englewood Cliffs, NJ: Prentice-Hall, 1986.
- [12] R. Severns, G. Bloom, *Modern DC-DC Switchmode Power Converter Circuits*. Van Nostrand Reinhold, N.Y.1985.